Secondary-control-based harmonics compensation scheme for voltage- And current-controlled inverters in islanded microgrids

Mousavi, Seyyed Yousef Mousazadeh; Jalilian, Alireza; Savaghebi, Mehdi; Guerrero, Josep M.

Published in:
IET Renewable Power Generation

DOI (link to publication from Publisher):
10.1049/iet-rpg.2019.0782

Publication date:
2020

Document Version
Accepted author manuscript, peer reviewed version

A Secondary-Control-Based Harmonics Compensation Scheme for Voltage- and Current- Controlled Inverters in Islanded Microgrids

Seyyed Yousef Mosazade Mousavi [1], Alireza Jalilian [2,3], Mehdi Savaghebi[4], and Josep M. Guerrero[5]

[1] Faculty of Engineering & Technology, University of Mazandaran, Bobolsar, Iran
[2]Department of Electrical Engineering Iran University of Science and Technology, Tehran, Iran
[3] Center of Excellence for Power System Automation and Operation, Iran University of Science and Technology
[4] Electrical Engineering Section, Mads Clausen Institute, University of Southern Denmark, Odense, Denmark
[5] Department of Energy Technology, Aalborg University, Aalborg, Denmark

Abstract: In this paper, a coordinated control scheme is proposed for sharing harmonics compensation effort among Voltage and Current Controlled Mode (VCM and CCM) inverters in islanded microgrids. In this method, the voltage harmonics compensation of Sensitive Bus (SB) is achieved by using secondary control as well as virtual impedance and admittance loops in primary control of VCM and CCM units. The limited capacity of the inverter is taken into account for harmonics compensation. Photovoltaic (PV) systems are considered as CCM units. The harmonics compensation is mainly performed by VCM inverters. However, in order to prevent these units from overloading, the PV interfacing inverters (CCM units) are called to collaborate in harmonics compensation whenever needed. The results of simulation study in in Matlab/Simulink show the effectiveness of this method in coordination of CCM and VCM units.

1. Introduction

Voltage Source Inverters (VSIs) are widely utilized for integration of Distributed Generation units (DGs) including Renewable Energy Resources (RESs) to distribution systems and Microgrids (MG) [1-6]. The control approaches of the VSIs in an MG can be classified to Current and Voltage Control Modes (CCM and VCM) depending on the prime-mover type of DGs [7]. In an islanded MG, the interfacing inverters of some energy storage systems and dispatchable (controllable) DG units (e.g. micro turbines, fuel cell, etc.) are operated as VCM units while the interfacing inverters of intermittent RES-based DGs such as photovoltaic (PV) systems and wind turbines (WT) are controlled as CCM units [8-10]. In islanded MGs, the VCM units which are known as grid forming units are responsible of voltage and frequency regulation. The harmonics compensation in MGs by using the VCM units is proposed in [9]-[22]. These methods can be classified to local-data- [9-15] or communication-based compensation [16-21].

Virtual impedance is most commonly used local-data-based compensation method for VCM units [13]. Compensation based on measuring the sensitive load bus data and applying hierarchical communication-based control methods are proposed in [17] and [18-21], respectively. Using Secondary Control (SC) for voltage quality enhancement can increase the accuracy and effectiveness; however, a communication system is required. In [22] and [23], a coordinated control of VCM DG units and active power filters is proposed while a supervisory control scheme of VCM DG units and active power filter is proposed in [24], for power quality improvement of multi-area MG. In [9-24], only the VCM units are considered while in an MG, CCM inverters are also present; furthermore, the limited capacity of VCM units should be considered.

On other hand, the multifunctional CCM inverters are proposed for harmonics compensation in microgrids and distribution systems [25-31]. In [29] and [30], the harmonics compensation is achieved by direct compensation of the nonlinear load harmonic current. The methods of [28] and [29] can be applied only when nonlinear loads and DG interfacing inverters are near to each other. Using virtual impedance is proposed in [30] and [31] for harmonics compensation. In this method, harmonics compensation is achieved by measuring voltage and creating a low impedance path for harmonics current.

In [32], an SC-based coordinated control of VCM and CCM units is proposed. In this method, the limited capacity of inverters is not considered. In [33], the coordinated control of VCM and CCM units for harmonic and reactive power sharing based on local data is proposed. In this control method, capacitive virtual impedance and conductive virtual admittance are respectively used in VCM and CCM units for harmonics compensation. Although the limited capacity of the CCM inverters is taken into account, this limitation is not considered in [33] for VCM units. A unified voltage harmonics control method for coordinated harmonic

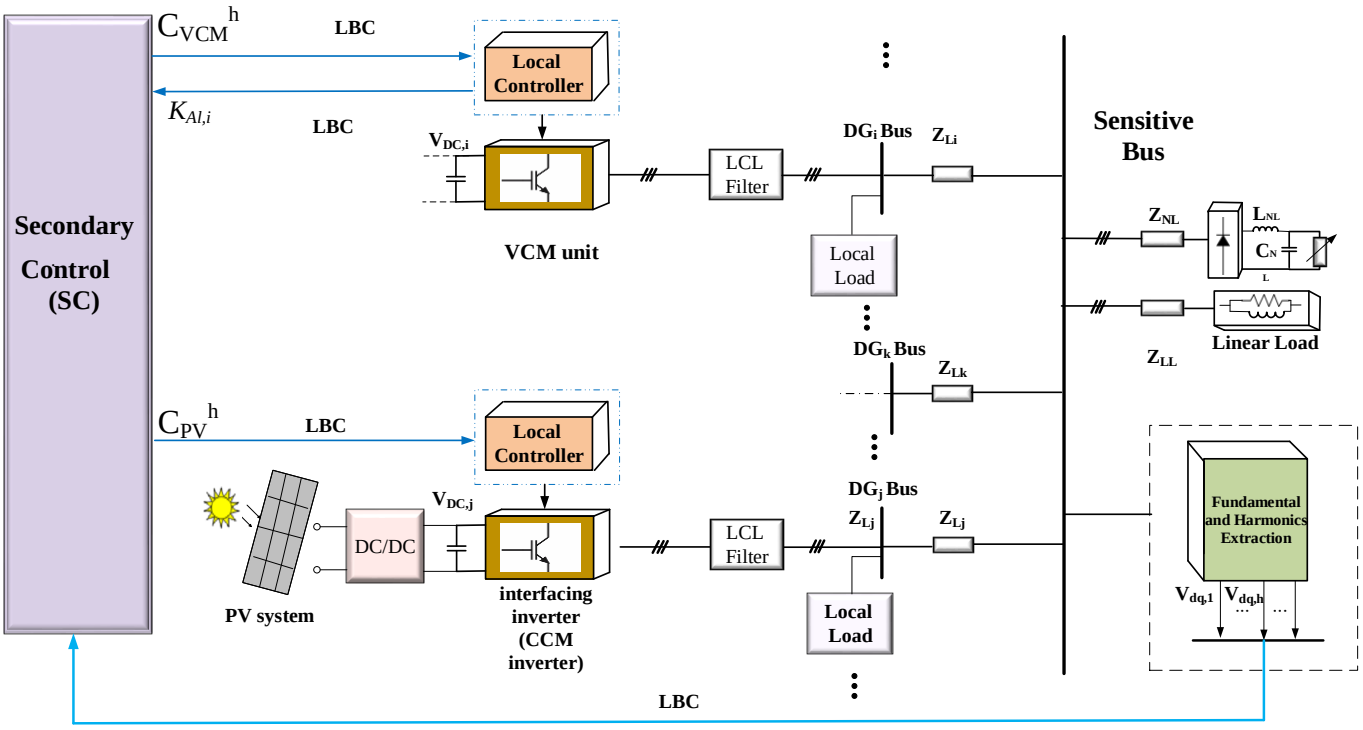

Fig. 1. General schematic of an MG with SC scheme for power quality enhancement

compensation of VCM and CCM inverters is proposed in [34] where similar to [33], the harmonics compensation of DG bus is achieved; however, in islanded microgrids, sensitive bus may be located relatively far from DG units.

In the present paper, in comparison to the methods presented in [10-23], CCM units are also considered and a coordinated control of VCM and CCM interfacing inverters are presented. The CCM units are fed by PV units. The VCM units are responsible of harmonics compensation in their normal situation. The harmonics sharing among these inverters is achieved by using resistive virtual impedance while the SC is used for harmonics compensation. As soon as any VCM inverter is overloaded, the existing PV multifunctional inverters as CCM units start to compensate harmonics in order to reduce the overload of VCM units; hence in comparison to [32] and [33], the limited capacity of both of CCM and VCM inverters is considered. The harmonic sharing of VCM units is achieved by virtual impedance which is a more common method for VCM than using virtual admittance proposed in [32]. Furthermore, in comparison to the methods proposed in [33] and [34] which are based on local measurement, the harmonics compensation of sensitive bus can be achieved. The change of sun irradiance and load is also investigated in this study. The main contributions of the paper can be listed as follow:

- Proposing a secondary-control-based coordinated control of CCM and VCM inverters.
- Considering the limited capacity of both VCM and CCM units while both sun irradiance and load may change.

The rest of the paper is organized as follows: In Section II, secondary-control-based power quality enhancement will be described. The control details of VCM and CCM (PV) units interfacing inverters will be presented in Section III. Section IV is dedicated to simulation results. Finally, the paper is concluded in Section V.

2. Secondary control based power quality enhancement

Fig. 1 shows the general scheme of an islanded MG with multifunctional DG interfacing inverters and communication-based SC. As depicted in this figure, DGs including VCM and CCM units are connected to DG buses and Sensitive Bus (SB) via their LCL filters and lines, respectively. For CCM units, PV system is used as prime mover; DC/DC boost converters are used for Maximum Power Point Tracking (MPPT) and stepping up PV output voltage. Nonlinear loads are also connected to DG terminals (Local Load) and sensitive buses. The fundamental and harmonic components of the SB voltage are extracted using the method described in [25]. The extracted data is transferred to SC via a low bandwidth communication (LBC) system. SC is used for power quality enhancement. For VCM units, the power quality enhancement comment (C_{VCM}^{h}) and overloading alert signal ($K_{AI,i}$) are transferred between VCM units and SC. As discussed later, $K_{AI,i}$ is used to inform SC about overloading of VCM units. The power quality enhancement comments of PV systems as CCM units (C_{PV}^{h}) are also transferred from SC to their control systems. The overloading limitation of CCM inverters are achieved in their control structure as mentioned in [25].

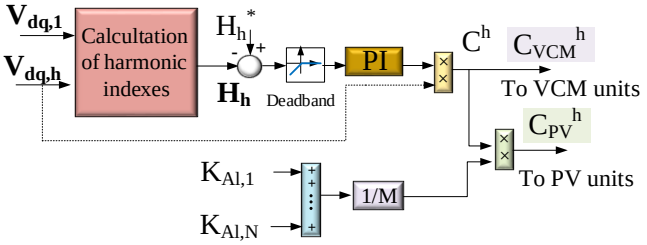

Fig. 2 Secondary control for coordinated control of VCM and CCM units in islanded microgrid.

As mentioned before, VCM units are expected to take part in compensation of power quality problems, too. Power quality enhancement occupies some part of VCM inverters capacity; hence, a coordinated control is required in order to prevent overloading of these units.

If VCM units reach to their full capacity, the CCM units will contribute in power quality enhancement in order to prevent the VCM units from overloading. In other words, the SC control system not only compensates the harmonics voltage of PCC but also can prevent the overloading of VCM units by CCM units harmonic compensation.

The architecture of SC is shown in Fig. 2. As depicted in this figure, harmonic index of each harmonic (H_h) is compared to the reference value (H_h^*) and the error is fed to a PI controller. A deadband block is utilized to prevent DG units from power quality enhancement when it is unnecessary, i.e. H_h is less than H_h^*. It should be mentioned that the value of H_h^* can be determined based on related standard or the desirable value of operator. In this condition, the harmonic compensation signals to both VCM and PV units ($C_{VCM}{}^h$ and $C_{PV}{}^h$) are zero. The outputs of PI controllers are multiplied to the respective harmonic voltages ($V_{dq,h}$). The data ($C_{VCM}{}^h$) is sent to VCM units for power quality enhancement.

$K_{Al,1}$,…, $K_{Al,N}$ show the status of the overcurrent problem of VCM units (subscript N denotes the number of VCM units). Fig. 3 depicts the variation of $K_{Al,i}$ as a function of a VCM inverter output current (I_{rms}) where $K_{Al,i}$ changes linearly from zero to 1 between rated current (I_r) and $1.2I_r$; hence the $K_{Al,i}$ =0 means that the overcorrect of VCM units does not happen while $K_{Al,i}$ =1 denotes that the current is equal or more than 120% of rated current. As shown in Fig. 2, if the values of all $K_{Al,i}$ are zero, compensation references of PV units ($C_{PV}{}^h$) will be zero. If one of VCM units are overloaded, this coefficients is increased and thus, PV units contribute in harmonics compensation. In Fig. 2, M denotes the number of CCM units.

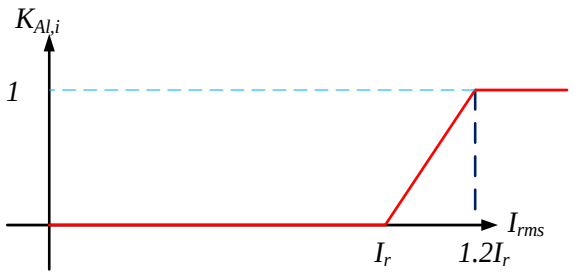

Fig. 3. $K_{Al,i}$ coefficient

3. Control of VCM and CCM inverters

The control and power stages of VCM and CCM units are depicted in Figs. 4(a) and 4(b), respectively.

A. VCM inverter

As depicted in Fig 4(a), the control scheme is implemented in αβ (stationary) frame. In MGs, VCM units are responsible of controlling voltage amplitude and frequency. In other words, the voltage amplitude and frequency of the MG is regulated by VCM inverter. The droop control which is expressed in following equation is widely used for VCM inverters [33]:

$$\omega = \omega_0 - m_p P,\ E = E_0 - n_p Q \qquad (1)$$

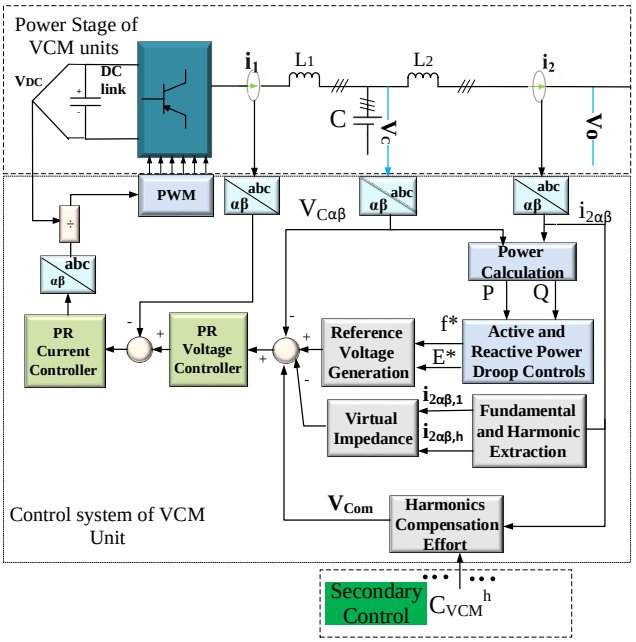

(a)

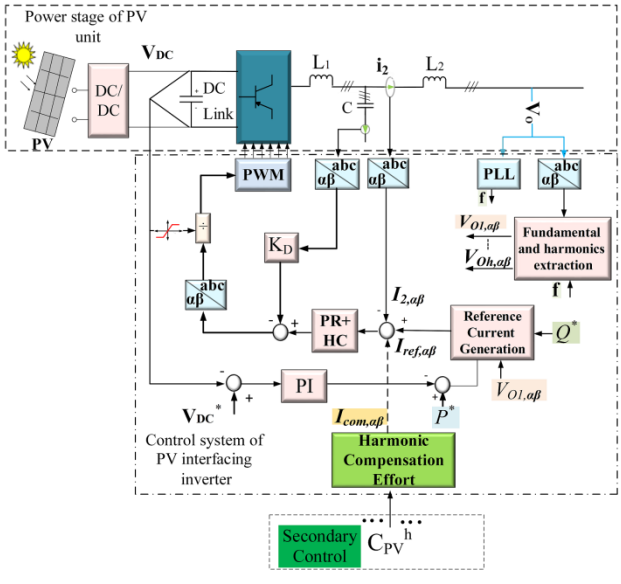

(b)

Fig. 4. Power and control stages of VCM and PV interfacing inverters: (a) VCM, (b) PV interfacing inverter (CCM)

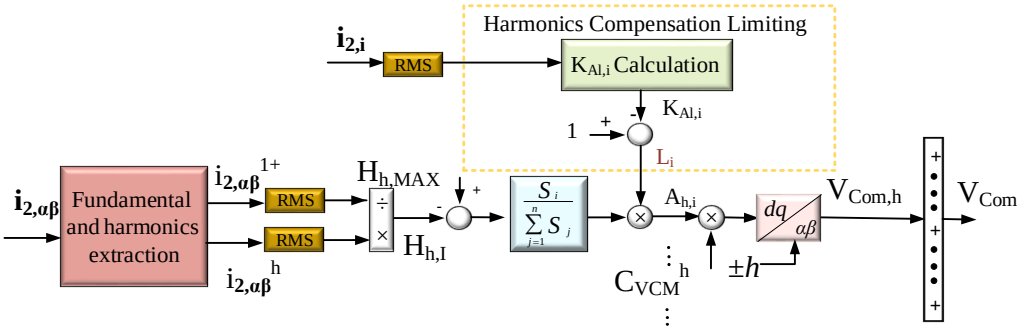

Fig. 5. Harmonics compensation effort block of VCM units.

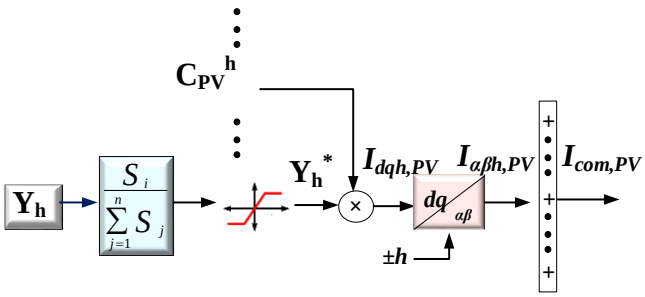

Fig. 6. Harmonics compensation block of PV interfacing inverters

where E_0 and E denote the rated and actual voltage amplitude values. ω_0 and ω are rated and actual angular frequencies. The proportional coefficients related to active and reactive powers droops are represented by m_p and n_p, respectively.

In this paper, inductive virtual impedance for fundamental frequency is used for decoupling power droops; furthermore, Virtual resistive impedances are utilized to share the nonlinear load current among DG units. Using resistive virtual resistances at harmonics frequencies increases harmonic distortion; however using SC can compensate the effect [23].

Fig. 5 shows the harmonic compensation effort block of the VCM unit. As depicted in this figure, after harmonics extraction, the harmonics indexes of DG current ($H_{h,I}$) are calculated. The resulted harmonic index is subtracted to its maximum value ($H_{h,MAX}$) in order to create a droop characteristics for harmonics compensation effort among DG units and it is not similar to error calculation we usually have before PI controllers. The DG units can contribute more in harmonic compensation if the difference of harmonics indexes and its maximum value is high. In order to share the compensation effort of VCM inverter according to their rated apparent power, the resulted signal is multiple to the ratio of rated capacity of the DG (S_i) to overall capacity of DGs ($\sum S_j$). The overload alert signal ($K_{Al,i}$) is calculated according to Fig. 3 and is subtracted to 1 (1- $K_{Al,i}$) in order to create the harmonics compensation limitation signal (L_i). If the overloading happens, the amount of $K_{Al,i}$ will increase and as a result, the value of L_i will decrease; hence, the harmonics compensation effort of this DG will decrease. On the other hand, if the DG does not face overcurrent problem, the value of Li is 1 ($K_{Al,i}$ =0) and the DG unit contributes in harmonics compensation with its maximum capacity. If the L_i is zero, according to Fig. 5, the DG cannot contribute in harmonic compensation to prevent the DG unit from overloading. After that, the resultant signal ($A_{h,i}$) is multiplied to the signal $C_{VCM}{}^h$ received from secondary control. Then, a dq/αβ transformation is applied. Finally, compensation reference signals ($V_{Com,h}$) in different frequencies are added to form the compensating voltage (V_{Com}).

B. CCM inverter

Since CCM inverter is connected via an LCL filter as depicted in Fig. 4(b), resonance damping is required [35] and [36]. In this paper, the active damping is implemented by using the capacitor current feedback with the damping gain K_D [37] and [38].

The PV model proposed in [39] is used in this study. The PV system is connected to the DC link of inverter by using a DC/DC converter. The MPPT is implemented by using Perturb and Observe (P&O) algorithm [40, 41]. The DC link voltage is controlled by using a Proportional-Integral (PI) controller. Proportional-Resonant (PR) controllers are used for tracking harmonics and fundamental component of current. The PR controllers are tuned at fundamental, fifth and seventh order harmonic frequencies.

Fig. 6 shows the harmonics compensation block of PV interfacing inverters. In this figure, the virtual admittance (conductance) at h^{th} harmonic is represented by Y_h. The gain $S_i/\sum S_i$ is used in order to share harmonics compensation effort according to the power capacities of the units. A saturation block is used to limit the virtual admittance for preventing DG units from over current. The maximum values of the virtual admittance are calculated based on the method presented in [33]. Then, the obtain signal (Y_h^*) is multiplied by the compensation reference from secondary control ($C_{PV}{}^h$). Afterward, the compensation current in dq form at h^{th} harmonic frequency ($I_{dqh,PV}$) should be transferred to αβ frame ($I_{\alpha\beta h,PV}$). Finally, compensating currents in different frequencies ($I_{\alpha\beta h,PV}$) are added to generate compensation current ($I_{Com,PV}$) .

4. Simulation Study

The system which is depicted in Fig. 7 is used for simulation study. Four DG units including two VCM and two PV units (CCM units) are used. The parameters of the power stage, PV and control systems are listed in 1, 2 and 3,

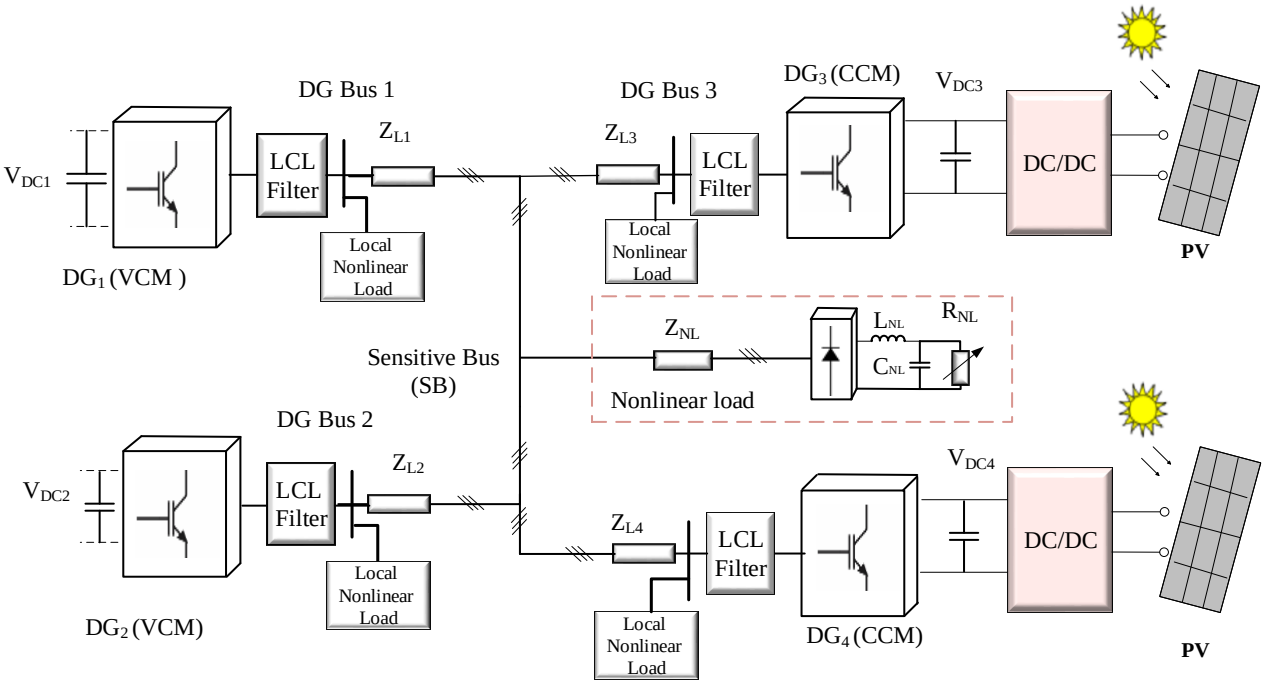

Fig. 7. Test system

Table 1. Parameters of power system

DC link voltage			LCL filter (L_1/C/L_2)		Voltage/ Frequency
650V			For all DGs: 8.6mH/4.5μF/1.8mH		230V/50Hz
Local Nonlinear Loads			SB Nonlinear Load		
C_{NL}(μF)	R_{NL}(Ω)	L_{NL}(mH)	C_{NL}(μF)	R_{NL}(Ω)	L_{NL}(mH)
235	114	0.084	235	50	0.084
Line impedance					
Z_{L1}(Ω)	Z_{L2}(Ω)	Z_{L3}(Ω)	Z_{L4}(Ω)		Z_{NL} (Ω)
0.1+0.5j	0.1+0.5j	0.1+0.5j	0.2+j		0.1+0.5j

Table 2. Parameters of PV system [34]

Definition	*Symbol*	*Value*
Number of series cells	N_S	56
Number of parallel cells	N_P	1
Temperature coefficient	K_I	0.0032
Open circuit voltage in normal condition	V_{OC}	33
Short circuit current	I_{SC}	8.214
Reference temperature	T_{ref}	25
Parallel resistance	$R_{SH,cell}$	415
Series resistance	$R_{S,cell}$	0.221
Ideality factor	m	3.3

Table 3. Control system parameters

Virtual admittance For CCM (PV) units	Desirable (reference) value of harmonics	Virtual impedance for VCM units
Y_{h5}, Y_{h7}, Y_{h11}	H_5^*, H_7^*	Z_{V1}, Z_{V5}, Z_{V7}
0.0025, 0.0025, 0.0025	0.5, 0.5	1j, 3, 3
DC link voltage controller		VCM harmonics compensation effort block
V_{DC}^*, *kp*, *ki*		$H_{5,MAX}$, $H_{7,MAX}$
650, 0.002, 0.005		1,1

respectively. The rated currents of VCM units are assumed to be 5 A; furthermore, the rated apparent powers of the PV interfacing inverters are 1650 VA.

In order to evaluate the proposed method, the following scenario is used:

Step 1 (3s⩽t<6s): Activation of virtual impedance without SC

Step 2 (6s⩽t<9s): Activation of SC without considering the CCM units compensation

Step 3 (9s⩽t<12s): Decreasing the power generated by PV system

Step 4 (12s ⩽ t<16s): Activation of secondary control considering the limited capacity of VCM inverter

Step 5 (16s⩽t⩽20s): Decreasing the load

Fig. 8 shows the active power delivered by VCM units. Since the rating capacities of these units are the same, equal droop coefficients are used for these units and as a result, their delivered active powers are equal in different steps. This figure depicts that when the powers of PV systems are decreased in Step 3, the VCM units deliver more power in order to regulate the frequency of the MG and in Step 5, and the delivered active powers of the VCM units are decreased.

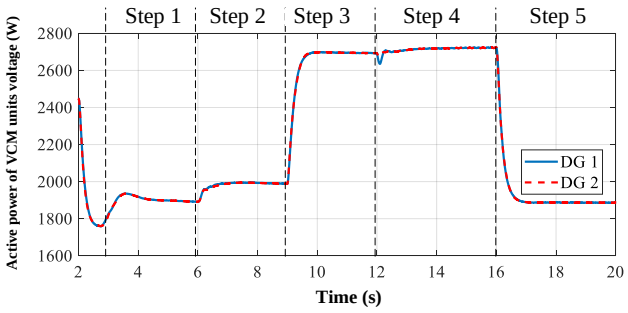

Fig. 8. Delivered active power of VCM units.

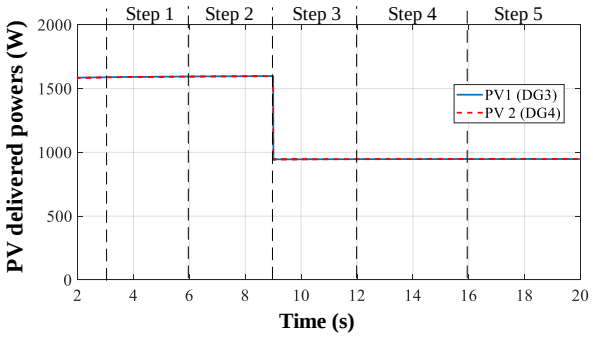

Fig. 9. Delivered active power of PV unit.

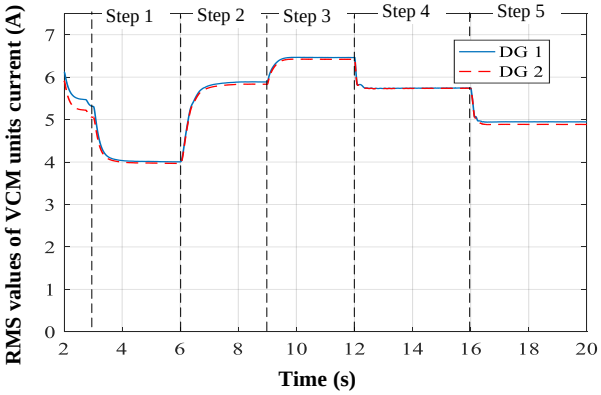

Fig. 10. Delivered currents of VCM units

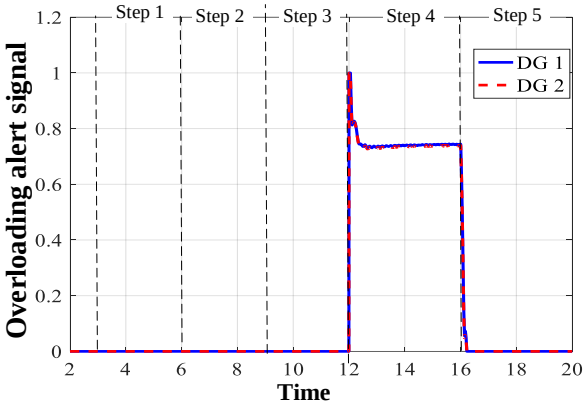

Fig. 11. The values of $K_{Al,1}$ and $K_{Al,2}$ of VCM units in different steps

Fig. 9 shows the active power delivered by PV interfacing inverters. As depicted in this figure, after changing the sun irradiance from 1000 Watt/m^2 to 600 Watt/m2 the MPPT and control systems of PV units can track the change.

Figs. 10 and 11 show the RMS value of VCM units currents and their over loading alert coefficients ($K_{Al,1}$ and $K_{Al,2}$), respectively. As depicted in Fig. 10, when the sun irradiance is changed from 1000 Watt/m^2 to 600 Watt/m^2 in Step 3, the RMS values of VCM currents are increased. Since the RMS values of these currents are more than 5 A in this Step, the amounts of $K_{Al,1}$ and $K_{Al,2}$ are increased after considering the limited capacity of these inverters in Step 4. Increasing $K_{Al,1}$ and $K_{Al,2}$ leads to contribution of PV interfacing inverter into harmonics compensation and reduced compensation efforts of VCM. As a result, the overcurrent problem of VCM units is mitigated as it is shown in Fig. 10. Finally after decreasing the load in Step 5, since the required load is decreased, the RMS values of VCM units are decreased. In this condition, since the VCM units do not face the overload problem, the $K_{Al,1}$ and $K_{Al,2}$ are 0 (i.e. L_1 and L_2 are 1) and they contribute in harmonics compensation with their full capacity.

The injected current of the PV interfacing inverters is also depicted in Fig. 12 for Steps 2, 4 and 5. As shown in this figure, since the values of $K_{Al,1}$ and $K_{Al,2}$ are 0 in Steps 2 and 5, the PV interfacing inverters do not contribute to harmonics compensation while in Step 4, they make an effort for compensation in order to mitigate the overload problem of VCM units.

Fig. 13 shows the fifth and seventh harmonics of SB. As mentioned before, since resistive virtual impedance is used for VCM units, the amounts of these harmonic components of SB bus are increased in Step 1. After secondary control activation in Step 2 the fifth and seventh orders harmonics of SB voltage are decreased and can track the reference (desirable) value 0.5% which is defined in Table. 3 (i.e. $H_5^* = H_7^* = 0.5\%$).

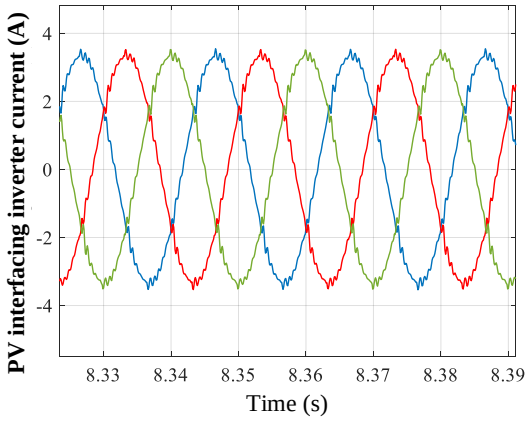

(a)

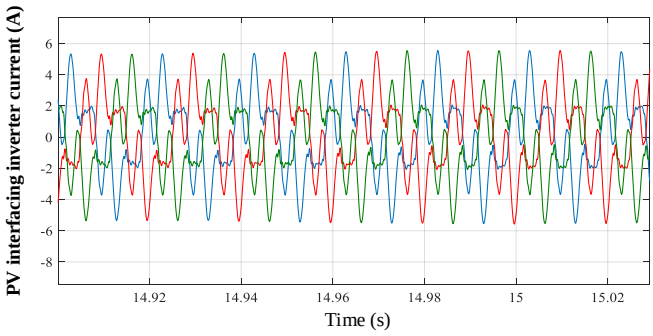

(b)

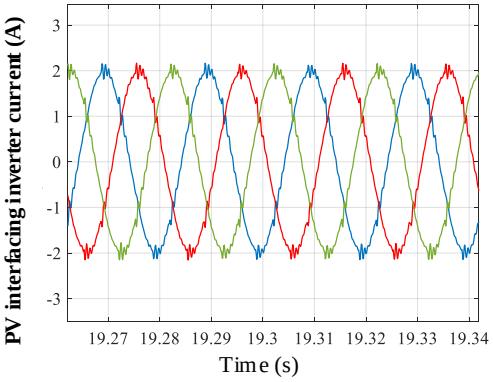

(c)

Fig. 12. Injected currents of PV interfacing inverters in different steps: a) Step 2, b) Step 4, c) Step 5

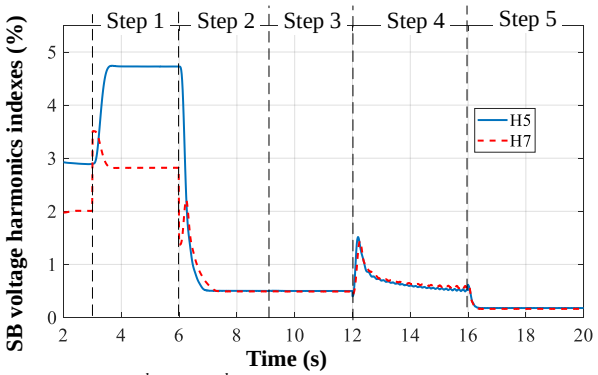

Fig. 13. 5th and 7th harmonics order of SB voltage.

5. Conclusions

In this paper, a coordinated secondary-control-based method is proposed for VCM and CCM units in an islanded microgrid. In this approach, the VCM units are responsible of power quality compensation as well as supporting frequency and voltage; however, the PV interfacing inverters contribute to harmonics compensation when VCM units are overloaded due to compensation. Simulation results showed that by using the secondary control approach, the overloading problem of VCM units is solved by harmonics contribution of CCM units.

Furthermore, the results showed that by using the secondary control, harmonics compensation is achieved and SB fifth and seventh orders harmonic voltages is reduced to approximately 0.5% which is defined as desirable values., so long as they follow the same style.

Reference

[1] J.M. Maza Ortega, A. Gomez Exposito, M. Barragan Villarejo, et al. “Voltage source converter-based topologies to further integrate renewable energy sources in distribution systems”, IET Renew. Power Gener., vol. 6, no.6, pp. 435–445, 2012.

[2] F. Blaabjerg, Z. Chen; S. B Kjaer, “Power electronics as efficient interface in dispersed power generation systems,” IEEE Trans. Power Electron., vol. 19, no. 5, pp. 1184-1194, Sept. 2004.

[3] A. Arzani, G.K. Venayagamoorthy, “Computational approach to enhance performance of photovoltaic system inverters interfaced to utility grids”, IET Renew. Power Gener. , vol. 12, pp. 112–124, 2018,

[4] T. Adefarati and R. C. Bansal, “Integration of renewable distributed generators into the distribution system: a review” IET Renew. Power Gener., vol. 10, no.7, pp. 873-884, 2016.

[5] A. Azghandi, S. M. Barakati, B. Wu, “Dynamic Modeling and Control of Grid-Connected Photovoltaic Systems based on Amplitude-Phase Transformation”, IJEEE, vol.14, no.4, pp:342-352, 2018.

[6] Z. Zeng, X. Li, and W. Shao, "Multi-functional grid-connected inverter: upgrading distributed generator with ancillary services," IET Renewable Power Generation, vol. 12, no. 7, pp. 797-805, 2018.

[7] J. Rocabert, A. Luna, F. Blaabjerg, P. Rodriguez, “Control of power converters in AC microgrids,” IEEE Trans. Power Electron., vol. 27, no. 11, pp. 4734-4749, Nov. 2012.

[8] D. Wu, F. Tang, T. Dragicevic, J. C. Vasquez and J. M. Guerrero, “A control architecture to coordinate renewable energy sources and energy storage systems in islanded Microgrids,” IEEE Trans. Smart Grid, vol. 6, no. 3, pp. 1156-1166, May 2015.

[9] I. Serban, C. Marinescu, "Control strategy of three-phase battery energy storage systems for frequency support in microgrids and with uninterrupted supply of local loads,", IEEE Trans. Power Electron., vol. 29, no. 9, pp. 5010-5020, Sept. 2014.

[10] Hajizadeh, A., Golkar, M.A.: ‘Fuzzy neural control of a hybrid fuel cell/ battery distributed power generation system’, IET Renew. Power Gener., 2009, 3, (4), pp. 402–414.

[11] S.Y. Mousazadeh Mousavi; A. Jalilian; M. Savaghebi; J. M. Guerrero, “Flexible Compensation of Voltage and Current Unbalance and Harmonics in Microgrids,” Energies, Vol. 10, 1568, 2017.

[12] M. Savaghebi, Q. Shafiee, J. C. Vasquez and J. M. Guerrero, "Adaptive virtual impedance scheme for selective compensation of voltage unbalance and harmonics in microgrids," IEEE Power & Energy Society General Meeting, Denver, CO, pp. 1-5, 2015.

[13] X. Wang, F. Blaabjerg, and Z. Chen, “Synthesis of variable harmonic impedance in inverter-interfaced distributed generation unit for harmonic resonance damping throughout a

distribution network," IEEE Trans. Ind. Appl., vol. 48, no. 4, pp. 1407-1417, Jul./Aug. 2012.
[14] A. Micallef; M. Apap; C. Spiteri-Staines; J. M. Guerrero, "Mitigation of harmonics in grid-connected and islanded microgrids via virtual admittances and impedances," IEEE Trans. Smart Grid, vol. 8, no.2, pp. 651-661, 2017
[15] Xiongfei Wang; Blaabjerg, F.; Zhe Chen, "Autonomous control of inverter-interfaced distributed generation units for harmonic current filtering and resonance damping in an islanded microgrid," IEEE Trans. Ind. Appl., vol. 50, no. 1, pp. 452-461, Jan.-Feb. 2014.
[16] R. Ghanizdeh and G. B. Gharehpetian, "Voltage quality and load sharing improvement in islanded microgrids using distributed hierarchical control", IET Renewable Power Generation, vol. 13, no. 15, pp. 2888-2898, 2019.
[17] Mehdi Savaghebi, Juan C. Vasquez, Alireza Jalilian, Josep M. Guerrero, Tzung-Lin Lee, Selective compensation of voltage harmonics in grid-connected microgrids, Mathematics and Computers in Simulation, Volume 91,2013 Pages 211-228,
[18] M. Savaghebi, A. Jalilian, J. C. Vasquez and J. M. Guerrero, "Secondary Control Scheme for Voltage Unbalance Compensation in an Islanded Droop-Controlled Microgrid," IEEE Transactions on Smart Grid, vol. 3, no. 2, pp. 797-807, June 2012.
[19] L. Meng et al., "Distributed Voltage Unbalance Compensation in Islanded Microgrids by Using a Dynamic Consensus Algorithm," IEEE Transactions on Power Electronics, vol. 31, no. 1, pp. 827-838, Jan. 2016.
[20] X. Wang, J. M. Guerrero, F. Blaabjerg and Z. Chen, "Secondary voltage control for harmonics suppression in islanded microgrids," 2011 IEEE Power and Energy Society General Meeting, San Diego, CA, 2011, pp. 1-8.
[21] M. Savaghebi; A. Jalilian; J. C. Vasquez; J. M. Guerrero, "Secondary control for voltage quality enhancement in microgrids," IEEE Trans Smart Grid, vol. 3, no. 4, pp. 1893-1902, Dec. 2012.
[22] M. M. Hashempour, M. Savaghebi, J. C. Vasquez and J. M. Guerrero, "A Control Architecture to Coordinate Distributed Generators and Active Power Filters Coexisting in a Microgrid," IEEE Transactions on Smart Grid, vol. 7, no. 5, pp. 2325-2336, Sept. 2016.
[23] M. M. Hashempour, M. Savaghebi, J. C. Vasquez and J. M. Guerrero, "Voltage unbalance and harmonic compensation in microgrids by cooperation of distributed generators and active power filters," 2016 7th Power Electronics and Drive Systems Technologies Conference (PEDSTC), Tehran, 2016, pp. 646-651.
[24] M. M. Hashempour, T. Lee, M. Savaghebi and J. M. Guerrero, "Real-Time Supervisory Control for Power Quality Improvement of Multi-Area Microgrids," IEEE Systems Journal, vol. 13, no. 1, pp. 864-874, 2019.
[25] Y. Naderi, S. H. Hosseini, S. Ghassem Zadeh, B. Mohammadi-Ivatloo, J. C. Vasquez, J. M. Guerrero, "An overview of power quality enhancement techniques applied to distributed generation in electrical distribution networks," Renewable and Sustainable Energy Reviews, Vol. 93, pp. 201-214, 2018.
[26] G.Todeschini, A.E. Emanuel, "Wind energy conversion systems as active filters: design and comparison of three control methods", IET Renew. Power Gener., vol. 4, no.4 , pp. 341–353, 2010
[27] Zeng, Z., Yang, H., Guerrero, J.M., et al.: 'Multi-functional distributed generation unit for power quality enhancement', IET Power Electron., 2015, 8, (3), pp. 467–476
[28] S. Y. Mousazadeh Mousavi, A. Jalilian, M. Savaghebi, J.M. Guerrero, "Power quality enhancement and power management of a multifunctional interfacing inverter for PV and battery energy storage system" Int. Trans. Electr. Energ. Syst. ;e2643, 2018.
[29] R. Noroozian, G. B. Gharehpetian, "An investigation on combined operation of active power filter with photovoltaic arrays," International Journal of Electrical Power & Energy Systems, Vol.46, pp. 392-399, 2013.
[30] S. Y. Mousazadeh Mousavi, A. Jalilian, M. Savaghebi, Josep M. Guerrero, "Coordinated control of multifunctional inverters for voltage support and harmonic compensation in a grid-connected microgrid," Electric Power Systems Research, Volume 155, Pages 254-264, 2018.
[31] Zheng Zeng; Rongxiang Zhao; Huan Yang, "Coordinated control of multi-functional grid-tied inverters using conductance a susceptance limitation," IET Power Electron, vol.7, no.7, pp.1821- 1831, July 2014.
[32] C. Blanco, D. Reigosa, J. C. Vasquez, J. M. Guerrero and F. Briz, "Virtual admittance loop for voltage harmonic compensation in microgrids," IEEE Trans. Ind. Appl., vol. 52, no. 4, pp. 3348-3356, July-Aug. 2016.
[33] S. Y. Mousazadeh Mousavi, A. Jalilian, M. Savaghebi and J. M. Guerrero, "Autonomous Control of Current and Voltage Controlled DG Interface Inverters for Reactive Power Sharing and Harmonics Compensation in Islanded Microgrids," IEEE Trans. on Power Elect., Early access, 2018.
[34] X. Zhao, L. Meng, C. Xie, J. M. Guerrero and X. Wu, "A Unified Voltage Harmonic Control Strategy for Coordinated Compensation With VCM and CCM Converters," IEEE Trans. on Power Elect., vol. 33, no. 8, pp. 7132-7147, Aug. 2018.
[35] Poh Chiang Loh and D. G. Holmes, "Analysis of multiloop control strategies for LC/CL/LCL-filtered voltage-source and current-source inverters," IEEE Trans Ind. Appl., vol. 41, no. 2, pp. 644-654, March-April 2005.
[36] Hisham Eldeeb, Ahmed Massoud, Ayman S. Abdel-Khalik, Shehab Ahmed, "A sensorless Kalman filter-based active damping technique for grid-tied VSI with LCL filter," International Journal of Electrical Power & Energy Systems, Volume 93, Pages 146-155, 2017,
[37] Ch. Bao, X. Ruan, X. Wang, W. Li, D. Pan, and K.Weng. "Step-by-Step Controller Design for LCL-Type Grid-Connected Inverter with Capacitor–Current-Feedback Active-Damping" IEEE Trans. Power Electron., vol. 29, no. 3, March 2014.
[38] M. Ben Saïd-Romdhane, M.W. Naouar, I. Slama-Belkhodja, E. Monmasson, cTime delay consideration for robust capacitor-current-inner-loop active damping of LCL-filter-based grid-connected converters," International Journal of Electrical Power & Energy Systems, Vol. 95, pp. 177-187, 2018.
[39] M. G. Villalva, J. R. Gazoli and E. R. Filho, "Comprehensive Approach to Modeling and Simulation of Photovoltaic Arrays," IEEE Transactions on Power Electronics, vol. 24, no. 5, pp. 1198-1208, May 2009.
[40] Nur Atharah Kamarzaman, Chee Wei Tan, "A comprehensive review of maximum power point tracking algorithms for photovoltaic systems Renewable and Sustainable Energy Reviews, Volume 37, Pages 585-598, 2014.
[41] A. K. Podder,; N. K. Roy, H. P. Roy, "MPPT methods for solar PV systems: a critical review based on tracking nature", IET Renewable Power Generation, Early access 2019.